

# NOVEL MEASUREMENTS OF PROTON STRUCTURE AT HERA

K.R. OLIVER (on behalf of the H1 and ZEUS collaborations)  
*Department of Physics, Denys Wilkinson Building, Keble Road,  
Oxford OX1 3RH, England*

ZEUS and H1 are multi-purpose detectors located on the HERA  $ep$  collider at DESY, Hamburg. Recent measurements of proton structure from both collaborations are presented, including the combination of early HERA data and associated PDF fit, measurement of high  $Q^2$  cross-sections and direct measurement of the structure function  $F_L$ .

## 1 HERA Combined Inclusive Cross Sections & QCD Fit

### 1.1 HERA Combined Cross Sections

Inclusive neutral current (NC) and charged current (CC) deep inelastic scattering (DIS) reduced cross sections were measured for unpolarised  $e^\pm p$  scattering by both collaborations during 1994-2000<sup>1</sup>. The kinematic range of the NC data in negative four-momentum-transfer squared,  $Q^2$ , and in Bjorken  $x$  was  $6 \cdot 10^{-7} \leq x \leq 0.65$  and  $0.045 \leq Q^2 \leq 30000 \text{ GeV}^2$  for values of inelasticity,  $y$ , between 0.005 and 0.95. The kinematic range of the CC data was  $1.3 \cdot 10^{-2} \leq x \leq 0.40$  and  $300 \leq Q^2 \leq 30000 \text{ GeV}^2$  for  $y$  between 0.037 and 0.76. Each experiment took about  $115 \text{ pb}^{-1}$  of integrated luminosity.

In order to combine the measurements from each collaboration, the measured reduced cross-sections were moved to a common  $Q^2$ - $x$  grid. Those points which were measured at  $p$ -beam energy of 820 GeV were moved to 920 GeV. Average values and uncertainties were then calculated. The combination method used was a  $\chi^2$  minimisation procedure which took into account the correlations of systematic uncertainties, resulting in an improved accuracy above that expected by doubling the statistics of the measurement. As two different detectors and different reconstruction methods were used, cross-calibration was possible. Similar systematic sources influenced the measured cross section differently as a function of  $x$  and  $Q^2$ . Therefore, requiring the cross sections to agree at all  $x$  and  $Q^2$  constrained the systematics efficiently. In total 1402 data points were combined to 741 cross-section measurements. The combination gave  $\chi^2/\text{NDF} = 637/656$ , showing that the data are consistent. Figure 1 shows the improvement in the uncertainties on the combined points relative to the uncertainties on the separate ZEUS and H1 measurements.

### 1.2 HERA QCD Fit

The combined data were the sole input in a NLO QCD analysis which determined a new set of parton distributions: HERAPDF1.0<sup>1</sup>. The low  $Q^2$  NC  $e^+p$  data determined the low- $x$  sea quark and gluon distributions. The high- $Q^2$  CC data, together with the difference between NC  $e^+p$  and  $e^-p$  cross sections at high  $Q^2$ , constrained the valence quark distributions. The use of the

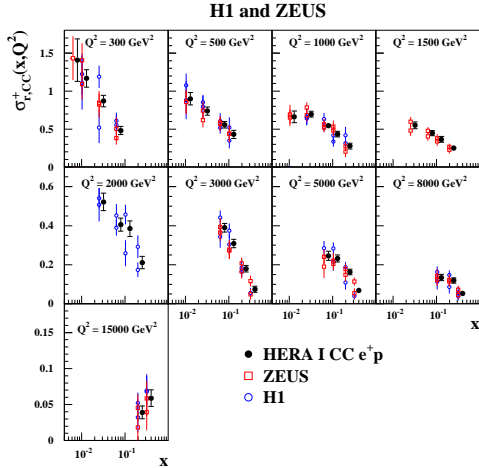


Figure 1: HERA combined CC  $e^+p$  reduced cross section (filled circles) as a function of  $x$  for 9  $Q^2$ -bins compared to the separate H1 (open circles) and ZEUS (open squares) data input to the averaging procedure.

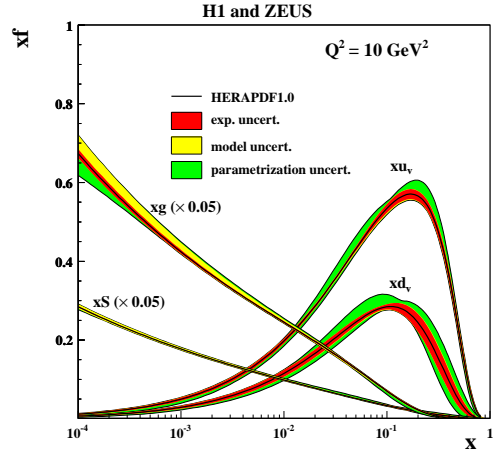


Figure 2: The HERAPDF1.0 PDFs (with experimental, model and parameterisation uncertainties) at  $Q^2 = 10 \text{ GeV}^2$ :  $xu_v$ ,  $xd_v$ ,  $xg$  and  $xS = 2x(\bar{u} + \bar{c} + \bar{d} + \bar{s} + \bar{b})$ .  $xg$  and  $xS$  are scaled down by a factor 20.

CC data allowed the down quark distribution in the proton to be determined without assuming isospin symmetry. In addition, the use of HERA data alone for the determination of parton distribution functions (PDFs) eliminated the need for heavy target corrections, which must be applied to DIS data from nuclear targets. The PDFs have small experimental uncertainties; an estimate of the model and parameterisation uncertainties of the fit result was also evaluated. A summary plot of the PDFs is shown in Figure 2. From Figure 3 it is clear that the HERA-I data used in deriving the fits had good sensitivity at low  $Q^2$  but limited statistical precision at high  $Q^2$ . Since HERA-II data is not yet included, further improvement is possible.

## 2 High- $Q^2$ Cross Sections

H1 recently made preliminary high- $Q^2$  CC<sup>2</sup> and NC<sup>3</sup> analyses using the complete HERA-II data set (collisions of unpolarised protons with polarised electron and positron beams in left and right helicity states).

The CC analysis includes measurement of the following polarised cross-sections: total cross-section; single differential cross-section in  $Q^2$ ; and the reduced cross-section. All were measured at two values of polarisation for each of the  $e^+p$  and  $e^-p$  data sets. The polarisation dependence of the charged current cross section has thus been established, extending previous tests of the chiral structure of the charged current interaction to high  $Q^2$ . The measurements are consistent with the absence of right handed charged currents.

The NC analysis includes measurement of the inclusive single differential cross section  $d\sigma/dQ^2$  and the reduced double differential cross section for the process  $e^\pm p \rightarrow e^\pm X$  for interactions with longitudinally polarised lepton beams. The data are consistent with the expected  $Q^2$  dependence of polarised cross sections. A measurement of the polarisation asymmetry as a function of  $Q^2$  was also made and agreed with the expectation. The cross sections were combined with previously published data from H1 to obtain the most precise unpolarised measurements. These were used to extract the structure function  $xF_3^{\gamma Z}$ .

Figure 4 shows the measurement of CC and NC single differential cross-sections in  $Q^2$  for

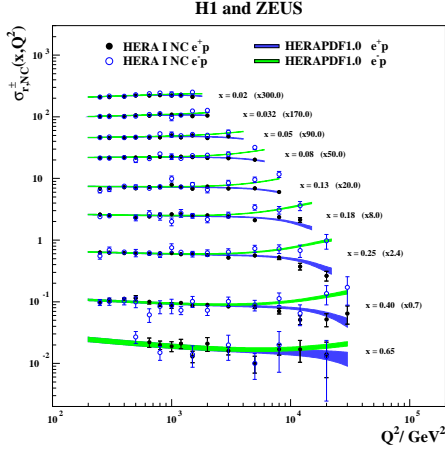


Figure 3: HERA combined NC  $e^+p$  reduced cross sections at high  $Q^2$ . The HERAPDF1.0 fit is superimposed. The bands represent the total uncertainty of the fit.

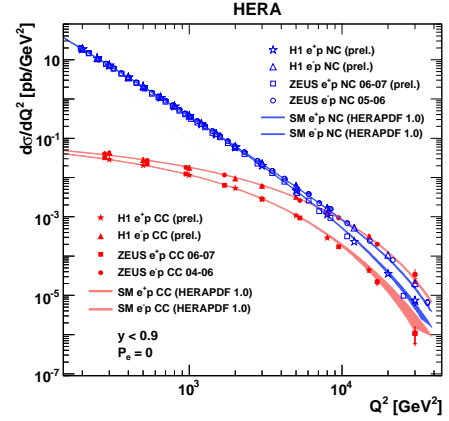


Figure 4: The unpolarised NC and CC cross sections  $d\sigma/dQ^2$ , shown for  $e^+p$  (open points) and  $e^-p$  (solid points) data from H1 and ZEUS. The inner (outer) error bars represent the statistical (total) errors.

$e^+p$  and  $e^-p$  data made by the ZEUS and H1 collaborations, including recently published data from ZEUS<sup>4 5</sup>.

### 3 HERA Combined Measurement of $F_L$

At low  $Q^2$ , the NC DIS reduced cross-section includes contributions from the structure functions  $F_2$  and  $F_L$  such that  $\sigma_r(x, Q^2) = F_2(x, Q^2) - y^2 / (1 + (1 - y)^2) F_L$ .  $F_L$  is only visible at high  $y$ . Direct measurement of  $F_L$  requires measurement of the reduced cross-sections at the same  $x$  and  $Q^2$  but different  $y$ , therefore cross-sections must be measured at different beam energies. H1<sup>6</sup> and ZEUS<sup>7</sup> measured the NC reduced cross-sections at low- $x$  and low- $Q^2$  at proton beam energies of 920 GeV (21.6 pb<sup>-1</sup>), 575 GeV (6.2pb<sup>-1</sup>) and 460 GeV (12.4 pb<sup>-1</sup>). The two collaborations have recently combined their separate measurements<sup>8 9</sup> to give the best-yet measurement of  $F_L$  from HERA. The combination procedure was based on that described in Section 1.1.

Figure 5 shows measurement of the cross-sections at the fixed  $x$  and  $Q^2$  at different beam energies. In Figure 6 these points are plotted as a function of  $y^2 / (1 + (1 - y)^2)$ . When plotted this way for given  $x$  and  $Q^2$ ,  $F_2$  is the intercept at the y-axis and  $F_L$  is the negative slope. The extraction of  $F_L$  in the region  $2.5 < Q^2 < 800$  GeV<sup>2</sup> is shown in Figure 7. The measurement is a new and important input to QCD fits because at NLO,  $F_L \propto \alpha_S x g(x, Q^2)$  and so the  $F_L$  measurement provides information about the gluon density of the proton.

### Acknowledgments

I am grateful to Hertford College, Oxford, and the Particle Physics sub-department at the University of Oxford for providing the financial support which enabled me to participate in the QCD and High Energy Interactions Session of the 2010 Recontres de Moriond.

### References

1. F. D. Aaron *et al.* H1 Collaboration and ZEUS Collaboration, JHEP **1001** (2010) 109 [arXiv:0911.0884].

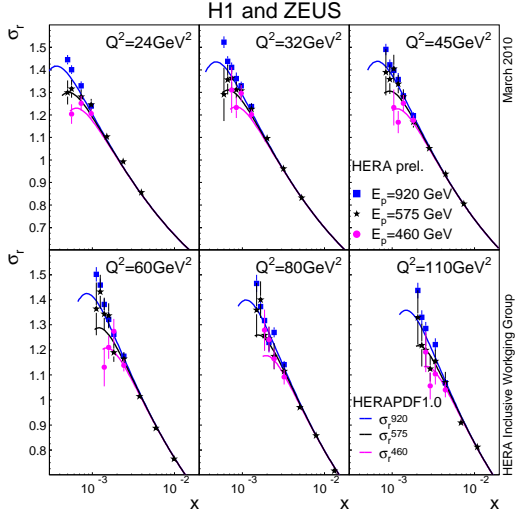


Figure 5: H1 and ZEUS average reduced cross section taken at proton beam energies,  $E_p$ , of 920 GeV (squares), 575 GeV (stars) and 460 GeV (circles). The error bars show total experimental uncertainties. Theoretical predictions from HERAPDF1.0 PDFs are shown as solid lines for 920 GeV (blue), 575 GeV (black) and 460 GeV (magenta).

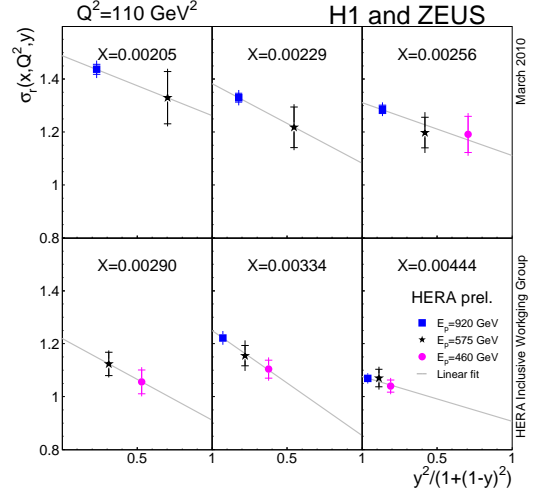


Figure 6: The reduced cross section measured at  $Q^2 = 110 \text{ GeV}^2$  and different  $x$  values as a function of  $y^2 / (1 + (1 - y)^2)$ . Measurements are taken at proton beam energies,  $E_p$ , of 920 GeV (squares), 575 GeV (stars) and 460 GeV (circles). The inner (full) error bars show the statistical (total) uncertainties. The lines show the linear fits used to determine  $F_L$ .

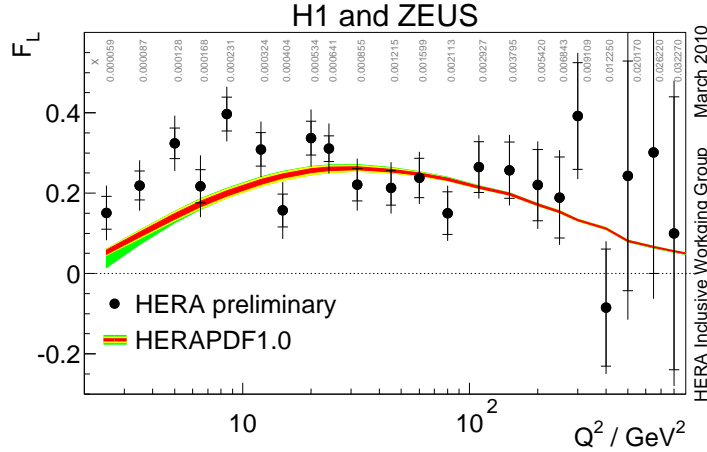


Figure 7: The structure function  $F_L$  averaged in  $x$  at given values of  $Q^2$  using combined H1 and ZEUS cross-section data. The resulting  $x$  values of the averaged  $F_L$  measurements are given in the figure for each point in  $Q^2$ . The inner (full) error bars are the statistical (total) uncertainties. The band represents the prediction from HERAPDF1.0 with parameterization (green) model (yellow) and experimental (red) uncertainties.

2. F.D. Aaron *et al.* H1 Collaboration (2009), [H1prelim-09-043].
3. F.D. Aaron *et al.* H1 Collaboration (2009), [H1prelim-09-042].
4. S. Chekanov *et al.* ZEUS Collaboration, Eur. Phys. J. C **61** (2009) 223 [arXiv:0812.4620].
5. S. Chekanov *et al.* ZEUS Collaboration, Eur. Phys. J. C **62** (2009) 625 [arXiv:0901.2385].
6. F. D. Aaron *et al.* H1 Collaboration, Phys. Lett. B **665** (2008) 139 [arXiv:0805.2809].
7. S. Chekanov *et al.* ZEUS Collaboration, Phys. Lett. B **682** (2009) 8 [arXiv:0904.1092].
8. F.D. Aaron *et al.* H1 Collaboration (2010), [H1prelim-10-043].
9. S. Chekanov *et al.* ZEUS Collaboration, (2010), [ZEUS-prel-10-001].